


Microparticles globally reprogram *Streptomyces albus* toward accelerated morphogenesis, streamlined carbon core metabolism, and enhanced production of the antituberculosis polyketide pamamycin

Martin Kuhl¹ | Lars Gläser¹ | Yuriy Rebets² | Christian Rückert³ |
Namrata Sarkar⁴ | Thomas Hartsch⁴ | Jörn Kalinowski³  | Andriy Luzhetskyy²  |
Christoph Wittmann¹ 

¹Institute of Systems Biotechnology, Saarland University, Saarbrücken, Germany

²Department of Pharmacy, Pharmaceutical Biotechnology, Saarland University, Saarbrücken, Germany

³Center for Biotechnology, Bielefeld University, Bielefeld, Germany

⁴Genedata GmbH, Munich, Germany

Correspondence

Christoph Wittmann, Institute of Systems Biotechnology, Saarland University, 66123 Saarbrücken, Germany.

Email: christoph.wittmann@uni-saarland.de

Funding information

Deutsche Forschungsgemeinschaft, Grant/Award Number: INST 256/418-1; Bundesministerium für Bildung und Forschung, Grant/Award Number: 031B0344

Abstract

Streptomyces spp. are a rich source for natural products with recognized industrial value, explaining the high interest to improve and streamline the performance of in these microbes. Here, we studied the production of pamamycins, macrodiolide homologs with a high activity against multiresistant pathogenic microbes, using recombinant *Streptomyces albus* J1074/R2. Talc particles (hydrous magnesium silicate, 3MgO·4SiO₂·H₂O) of micrometer size, added to submerged cultures of the recombinant strain, tripled pamamycin production up to 50 mg/L. Furthermore, they strongly affected morphology, reduced the size of cell pellets formed by the filamentous microbe during the process up to sixfold, and shifted the pamamycin spectrum to larger derivatives. Integrated analysis of transcriptome and precursor (CoA thioester) supply of particle-enhanced and control cultures provided detailed insights into the underlying molecular changes. The microparticles affected the expression of 3,341 genes (56% of all genes), revealing a global and fundamental impact on metabolism. Morphology-associated genes, encoding major regulators such as SsgA, RelA, EshA, Factor C, as well as chaplins and rodmins, were found massively upregulated, indicating that the particles caused a substantially accelerated morphogenesis. In line, the pamamycin cluster was strongly upregulated (up to 1,024-fold). Furthermore, the microparticles perturbed genes encoding for CoA-ester metabolism, which were mainly activated. The altered expression resulted in changes in the availability of intracellular CoA-esters, the building blocks of pamamycin. Notably, the ratio between methylmalonyl CoA and malonyl-CoA was increased fourfold. Both metabolites compete for incorporation into pamamycin so that the altered availability explained the pronounced preference for larger derivatives in the microparticle-enhanced process. The novel insights into the behavior

This is an open access article under the terms of the Creative Commons Attribution License, which permits use, distribution and reproduction in any medium, provided the original work is properly cited.

© 2020 The Authors. *Biotechnology and Bioengineering* published by Wiley Periodicals LLC

of *S. albus* in response to talc appears of general relevance to further explore and upgrade the concept of microparticle enhanced cultivation, widely used for filamentous microbes.

KEYWORDS

filamentous microbe, microparticle, morphogenesis, polyketide, *Streptomyces*, transcriptome

1 | INTRODUCTION

Streptomycetes are an important source of natural products for pharmaceutical, medical, agricultural, and nutraceutical application, including more than two-third of all known antibiotics of microbial origin (Bibb, 2013). Over the past, they have provided a range of industrialized blockbuster drugs, including streptomycin (Ehrlich, Bartz, Smith, Joslyn, & Burkholder, 1947), chloramphenicol (Ehrlich et al., 1947), candicidin (Lechevalier, Acker, Corke, Haenseler, & Waksman, 1953), doxorubicin (Arcamone et al., 1969), ivermectin (Campbell, Fisher, Stapley, Albers-Schönberg, & Jacob, 1983; Juarez, Scholnik-Cabrera, & Dueñas-Gonzalez, 2018), bialaphos (Bayer et al., 1972), and rapamycin (Sehgal, Baker, & Vézina, 1975; Vézina, Kudelski, & Sehgal, 1975), amongst others (Kieser, Bibb, Buttner, Chater, & Hopwood, 2000). It is easy to understand that strategies to activate and enhance the synthesis of natural products in Streptomycetes have been of a broad interest from early on and still display a topic of major relevance (Ahmed et al., 2020; Horbal, Marques, Nadmid, Mendes, & Luzhetskyy, 2018; Kallifidas, Jiang, Ding, & Luesch, 2018; Lopatniuk et al., 2019; Zhang et al., 2020).

Members of the genus are well known for a complex morphology linked to their multicellular life cycle, which starts with the germination of a single spore that grows into a vegetative mycelium by linear tip extension and hyphae branching (Chater & Losick, 1997; van Dissel, Claessen, & van Wezel, 2014), then forms an aerial mycelium, and finally differentiates into uninucleoid cells that further develop again into spores (Angert, 2005). In submerged culture, more relevant for industrial production, morphogenesis comprises primary and secondary mycelial networks, pellets, and sporulation (van Dissel et al., 2014).

Notably, morphological development and natural product formation are closely linked, and various efforts have been made to increase production through an altered morphology (Chater, 1984). Genetic perturbation, as an example, provided remarkable progress (van Dissel et al., 2014; Koebisch, Overbeck, Piepmeyer, Meschke, & Schrempf, 2009; van Wezel et al., 2006; Xu, Chater, Deng, & Tao, 2008). Other studies aimed to influence morphology on the process level, including the modification of agitation speed (Belmar-Beiny & Thomas, 1991; Xia, Lin, Xia, Cong, & Zhong, 2014), medium viscosity (O'Cleirigh, Casey, Walsh, & O'Shea, 2005), pH value (Glazebrook, Vining, & White, 1992), the addition of specific nutrients (Jonsbu, McIntyre, & Nielsen, 2002), and even subinhibitory antibiotic concentrations (Wang, Zhao, & Ding, 2017). These studies,

however, have revealed a mixed outcome and largely remained on a trial and error level.

Strikingly, a breakthrough in tailored control of morphology was achieved with the introduction of inorganic microparticles, added to the cultures (R. Walisko, Krull, Schrader, & Wittmann, 2012). Pioneering studies successfully used such materials to streamline the morphology of eukaryotic filamentous fungi and enhance the formation of enzymes (Driouch, Hänsch, Wucherpennig, Krull, & Wittmann, 2012; Driouch, Roth, Dersch, & Wittmann, 2010; Kaup, Ehrich, Pescheck, & Schrader, 2008), polyketides, and alcohols (Etschmann et al., 2015). More recently, several studies suggested that microparticles are also beneficial to enhance product formation in filamentous prokaryotes (Holtmann et al., 2017; Liu, Tang, Wang, & Liu, 2019; Ren et al., 2015; J. Walisko et al., 2017).

Here, we studied the use of talc microparticles for the production of pamamycins (Figure 1), a family of 16 macrodiolide homologs that are highly active against multiresistant pathogenic microbes, using recombinant *Streptomyces albus* J1074/R2 (Rebets et al., 2015). Carefully conducted cultures with analysis of growth, product formation and cellular morphology enabled us to specifically study the impact of the microparticle addition on production performance. In addition, transcriptome and intracellular CoA thioester analyses provided insights into the cellular response of *S. albus* and provided a systems-level picture on how the particles reprogrammed morphogenesis and streamlined metabolism for enhanced production and a notable shift toward heavier pamamycin homologs.

2 | MATERIALS AND METHODS

2.1 | Strain

S. albus J1074/R2 expressing the heterologous pamamycin gene cluster was obtained from previous work (Rebets et al., 2015). For strain maintenance, spores collected from agar plate cultures after 5-day incubation were resuspended in 20% glycerol and kept at -80°C .

2.2 | Media

Mannitol-soy flour agar contained per liter: 20 g mannitol (Sigma-Aldrich, Taufkirchen, Germany), 20 g soy flour (Schoenenberger

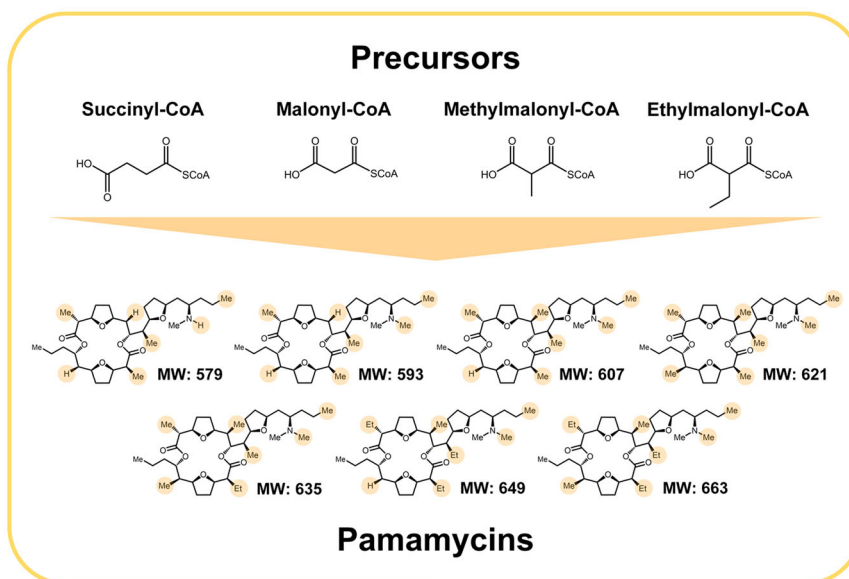


FIGURE 1 Chemical structure of the polyketide pamamycin family and the building blocks of its different derivatives succinyl-CoA, malonyl-CoA, methylmalonyl-CoA, and ethylmalonyl-CoA. The individual combination of different CoA-esters results in a different decoration of the product (-H, -CH₃, -C₂H₅) at specific positions and determines the molecular weight (MW). Except for Pam 607, several isomers exist for each pamamycin, differing by the exact position of the side chains (Hanquet, Salom-Roig, & Lanners, 2016). For every pamamycin mass derivative, one exemplary structure is shown [Color figure can be viewed at wileyonlinelibrary.com]

Hensel, Magstadt, Germany), and 20 g agar (Becton & Dickinson, Heidelberg, Germany). Liquid SGG medium was used for pre- and main cultures for pamamycin production and contained per liter: 10 g soluble starch (Sigma-Aldrich), 10 g glycerol, 2.5 g corn steep powder (Sigma-Aldrich), 5 g bacto peptone (Becton & Dickinson), 2 g yeast extract (Becton & Dickinson), 1 g sodium chloride, and 21 g MOPS. The pH of the medium was adjusted to 7.2, using 6 M NaOH. Talc microparticles (hydrous magnesium silicate, 3MgO·4SiO₂·H₂O, 10 μm; Sigma-Aldrich) were resuspended in 50 mM Na-acetate buffer (pH 6.5), autoclaved at 121°C for 20 min, and added to the sterile medium before inoculation of selected experiments (Driouch, Sommer, & Wittmann, 2010).

2.3 | Cultivation

One loop of spores was scratched from a 5-day old plate culture and used to inoculate a liquid preculture, which was then grown overnight in a 500-ml baffled shake flask with 50 ml medium and 30 g soda-lime glass beads (5 mm; Sigma-Aldrich). When the preculture reached the late exponential phase, an appropriate amount of cells was collected (8,500g, room temperature, 5 min), resuspended in 10 ml fresh medium, and used to inoculate the main-culture (50 ml medium in 500-ml baffled shake flasks). Main cultures (with and without talc) were inoculated from the same preculture to enable identical starting conditions. All cultivation experiments were conducted in triplicate on a rotary shaker (28°C, 230 rpm, 75% relative humidity, 5-cm shaking diameter, Multitron, Infors AG, Bottmingen, Switzerland).

2.4 | Quantification of cell concentration

The cell dry weight (CDW) of *S. albus* was measured as follows. Cells were collected (10,000g, 4°C, 10 min), washed twice with 15 ml deionized water and freeze-dried. Subsequently, the CDW was gravimetrically determined (Gläser et al., 2020). In microparticle cultivations, the measurements were corrected for the added talc (Driouch, Sommer, et al., 2010). The optical density (OD₆₀₀) of a culture was measured at 600 nm (UV-1600PC spectrophotometer; VWR, Hannover, Germany). Individual correlations allowed to infer the CDW from optical density measurement for different talc concentrations: CDW (g/L) = 0.64 × OD₆₀₀ (control), CDW (g/L) = 0.70 × OD₆₀₀ (2.5 g/L talc), CDW (g/L) = 0.76 × OD₆₀₀ (10 g/L talc; Figure S8), as described before (Becker, Klopprogge, Schröder, & Wittmann, 2009). All measurements were performed in triplicate.

2.5 | Quantification of substrates

Before analysis, starch was hydrolyzed to glucose monomers for 3 hr using 3 M HCl at 100°C. Glucose and glycerol were quantified by high-performance liquid chromatography (HPLC; 1260 Infinity Series; Agilent, Waldbronn, Germany) using an Aminex HPX-87H column (300 × 7.8 mm; Bio-Rad, München, Germany) and 7 mM H₂SO₄ as mobile phase (55°C, 0.7 ml/min). Refraction index measurement was used for detection and external standards were used for quantification. Phosphate was analyzed by HPIC (Dionex Integriion; Thermo Fisher Scientific, Karlsruhe, Germany) using a Dionex IonPac AS9-HC column (2 × 250 mm; Thermo Fisher Scientific) and 9 mM Na₂CO₃ as

mobile phase (35°C, 0.25 ml/min). Conductivity measurement was used for detection and an external standard was used for quantification. All measurements were performed in triplicate.

2.6 | Morphology analysis

Five microliter culture broth was transferred onto a glass for bright-field microscopy (Olympus IX70 microscope, Hamburg, Germany). The software ImageJ 1.52 (Schneider, Rasband, & Eliceiri, 2012) was used to automatically determine the size of pellets formed during growth (Krull et al., 2013). The diameter of a pellet was assumed as the smallest circle into which the complete aggregate fitted (Martin & Bushell, 1996). At least 150 aggregates were analyzed per sample.

2.7 | Natural compound extraction and quantification

Pamamycin was extracted from culture broth using a two-step process. First, 200 μ l broth was mixed with 200 μ l acetone and incubated for 15 min (1,000 rpm, room temperature, Thermomixer F1.5; Eppendorf, Wesseling, Germany). Subsequently, 200 μ l ethyl acetate was added, and the mixture was incubated for further 15 min under the same conditions. Afterward, the organic phase was collected (20,000g, room temperature, 5 min). The solvents were evaporated under a laminar nitrogen stream. The extract was redissolved in 2 ml methanol, clarified from debris (20,000g, 4°C, 10 min) and analyzed, using HPLC-ESI-MS (Agilent Infinity 1290, Waldbronn, Germany; AB Sciex QTrap 6500, Darmstadt, Germany). The different pamamycin derivatives (Figure 1) were separated on a C18 column (Vision HT C18 HighLoad, 100 \times 2 mm, 1.5 μ m, Dr. Maisch, Ammerbuch-Entringen, Germany) at a flow rate of 300 μ l/min (8 mM ammonium formate in 92% acetonitrile) and 45°C. Detection was carried out in positive selected ion monitoring mode, using the corresponding $[M+H]^+$ ion for each derivative (Figure 1). All measurements were performed in triplicate.

2.8 | Extraction and quantification of intracellular CoA-esters

The analysis of CoA-esters was conducted as recently described (Gläser et al., 2020). In short, a broth sample (8 mg CDW) was transferred into a precooled tube, which contained quenching and extraction solution (95% acetonitrile, 25 mM formic acid, -20°C) at a volume ratio of 1:4 followed by repetitive mixing and cooling on ice for 10 min, clarification from cell debris (15,000g, 4°C, 10 min) and the addition of 10 ml supercooled deionized water. The cell pellet was washed twice with 8 ml supercooled deionized water. All supernatants were combined, followed by freezing in liquid nitrogen and lyophilization. Before analysis, the obtained dry extract was dissolved in 500 μ l precold buffer (25 mM ammonium formate, 2% methanol, pH 3.0, 4°C) and filtered

(Ultrafree-MC 0.22 μ m; Merck, Millipore, Germany). Analysis of the CoA-esters was performed on a triple quadrupole MS (QTRAP 6500+; AB Sciex, Darmstadt, Germany) coupled to an HPLC system (Agilent Infinity 1290 System). Separation of the analytes of interest was conducted at 40°C on a reversed phase column (Gemini 100 \times 4.6 mm, 3 μ m, 110 Å, Phenomenex, Aschaffenburg, Germany) using a gradient of formic acid (50 mM, adjusted to pH 8.1 with 25% ammonium hydroxide, eluent A) and methanol (eluent B) at a flow rate of 600 μ l/min. The fraction of eluent B was as follows: 0–12 min, 0–15%; 12–16 min, 15–100%; 16–18 min, 100%; 18–20 min, 100–0%; 20–25 min, 0%. The first 3 min of the analysis were discharged to minimize the entry of salts into the mass spectrometer. CoA-esters of interest were analyzed in positive ionization mode, using multiple reaction monitoring. Analyte specific instrument settings such as declustering potential, collision energy, and collision cell exit potential were individually optimized for each CoA-ester, using synthetic standards. All measurements were done in triplicate.

2.9 | Transcriptome analysis

Cells (1 ml broth) were collected by centrifugation (20,000g, 4°C, 1 min) and immediately frozen in liquid nitrogen. RNA was extracted with the Qiagen RNA Mini Kit (Qiagen, Hilden, Germany) according to the manufacturer's instructions. Residual DNA was removed by digestion with 10 U RNase-free DNase I (Thermo Fisher Scientific) for 1 hr in the presence of RiboLock RNase inhibitor (Thermo Fisher Scientific). After DNA digestion, the RNA was again purified with the same kit. RNA quality was checked by Trinean Xpose (Gentbrugge, Belgium) and the Agilent RNA 6000 Nano Kit on an Agilent 2100 Bioanalyzer (Agilent Technologies, Böblingen, Germany). Ribosomal RNA molecules were removed from total RNA with the Ribo-Zero rRNA Removal Kit (Illumina, San Diego, CA) and removal of rRNA was checked with the Agilent RNA 6000 Pico Kit on an Agilent 2100 Bioanalyzer. Libraries of complementary DNA (cDNA) were prepared with the TruSeq Stranded mRNA Library Prep Kit (Illumina), and the resulting cDNA was sequenced paired end on an Illumina HiSeq 1500 system using 2 \times 75 bp read length. Reads were mapped to the *S. albus* J1074/R2 genome sequence (CP059254.1) with Bowtie2 using standard settings (Langmead & Salzberg, 2012) except for increasing the maximal allowed distance for paired reads to 600 bases. For visualization of read alignments and raw read count calculation, ReadXplorer 2.2.3 was used (Hilker et al., 2014). Due to a high un-specific background over both strands, the raw read count for each CDS was corrected by subtracting the length-adjusted median read count calculated over all CDS from the respective noncoding strand. Using the resulting data, DESeq2 (Love, Huber, & Anders, 2014) was used to QC the datasets via, among others, calculation of the sample to sample distances (Figure S9) and PCA (Figure S10). In addition, DESeq2 was used to calculate DGE datasets. Raw datasets (sequenced reads) as well as processed datasets (input matrix and normalized read counts from DESeq2) are available from GEO (GSE155008). For statistical analysis, Student's *t* test was carried out

and the data were filtered for genes with a \log_2 -fold change ≥ 1 ($p \leq 0.05$). Hierarchical clustering was conducted, using the software package gplots (R Core Team, 2014; Warnes, Bolker, Bonebakker, & Gentleman, 2016). For visualization, Voronoi tree maps were created, using the Voronoi tool (Santamaría & Pierre, 2012) for Java (version 8, update 231, Build 1.8.0_231-b11). RNA extraction and sequencing were conducted as biological triplicates, except for one of the controls, where one replicate was lost during processing. Given the excellent reproducibility of all analyzed samples (Figures S10 and S11), the available dataset was regarded acceptable to enable a robust and reliable evaluation of gene expression.

3 | RESULTS

3.1 | Pamamycin production in *S. albus* J1074/R2

In a first set of experiments, the pamamycin production performance of *S. albus* J1074/R2 was assessed in liquid SGG medium, which contained starch and glycerol as carbon source (Figure 2a). After inoculation, cells immediately started to grow into mycelial networks, which then aggregated into pellets as typically observed for actinomycetes. Growth

lasted for about 12 hr. The production of pamamycins started after ~ 9 hr at the end of the growth phase (when phosphate became limiting, Figure S11) and continued during the later stationary phase. The recombinant strain produced a rich spectrum of different pamamycins, which were attributed to derivatives with different side chains according to their molecular mass, that is, Pam 579, Pam 593, Pam 607, Pam 621, Pam 635, Pam 649, and Pam 663. Smaller pamamycins (Pam 579, Pam 593, and Pam 607) were most prominent. The total pamamycin titer was 18 mg/L. Interestingly, starch was the major carbon source until ~ 24 hr (Figure S11). Glycerol remained practically untouched during the initial process, but was consumed later when starch reached a lower level (although it was still present). During the cultivation, the pH value varied between 6.5 and 7.5. It decreased during the growth phase and increased again in later phases.

3.2 | The addition of talc to the culture of *S. albus* J1074/R2 increases the production of pamamycin up to threefold

S. albus J1074/R2, cultivated in SGG medium with microparticles (2.5 g/L talc), revealed an increased pamamycin titer of 22 mg/L

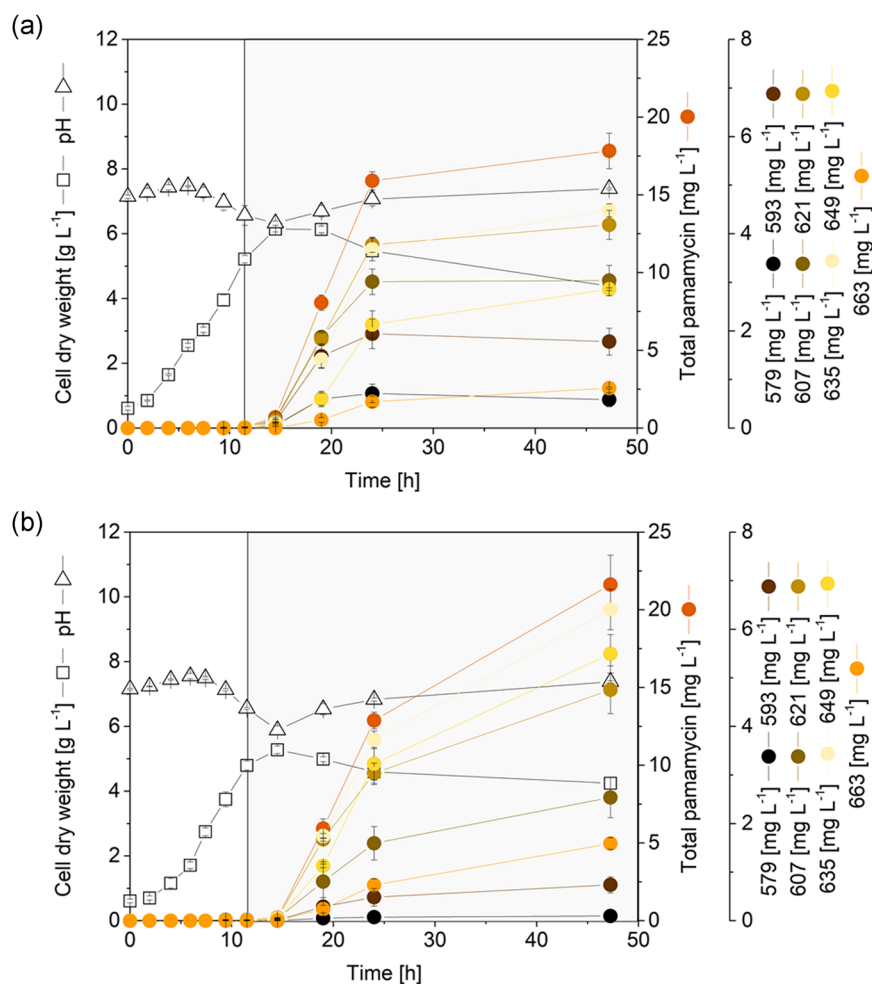


FIGURE 2 Impact of talc microparticles on growth and pamamycin production in *Streptomyces albus* J1074/R2 using complex SGG medium with starch and glycerol as main carbon source. (a) Control culture without microparticles. (b) Microparticle-enhanced culture with 2.5 g/L talc. Growth phase (white) and major pamamycin production phase (gray) are indicated by color [Color figure can be viewed at wileyonlinelibrary.com]

(Figure 2b). Interestingly, talc did not generally enhance production, but specifically affected the pamamycin spectrum. The titer of low molecular weight derivatives (Pam 579, Pam 593, Pam 607) was found reduced, whereas higher molecular weight pamamycins were increased (Pam 635, Pam 649, Pam 663). This effect was most prominent for the two heaviest pamamycins (Pam 649, Pam 663). These two derivatives were increased almost twofold. The presence of the talc particles resulted in a slightly faster use of phosphate (Figure S11). The mode of substrate utilization was the same as for the control, mainly starch consumption during the initial phase and activation of glycerol utilization after ~20 hr. Generally, glycerol uptake was more pronounced than in the control. It's uptake was faster, and a significantly lower amount of it was left at the end of the process (Figure S11). The pH profile was like the control.

Further studies revealed a strong impact of the amount of talc on the product level (Figure 3a). An optimum performance was observed for talc levels of 10 and 15 g/L. These concentrations provided 50 mg/L of total pamamycin. An even higher concentration of talc (20 g/L) resulted in a reduced titer (37 mg/L), slightly below the optimum. Notably, the stimulating effect of the microparticles on the formation of larger pamamycins was maintained even at the highest talc level: 20 g/L of talc specifically enhanced production of pamamycins Pam 649 and Pam 663. Altogether, a concentration of 10 g/L talc appeared optimal and was chosen for further studies.

3.3 | Talc microparticles reduce the pellet size of *S. albus* J1074/R2 more than sixfold

The addition of talc caused substantial changes in cellular morphology (Figure 3b). In control cultures without talc, the formed pellets exhibited an average diameter of ~435 μm . Already low levels of talc (2.5 g/L) led to a drastic decrease to 150 μm . With an increasing microparticle concentration, this effect was even more pronounced. The smallest pellet diameter (70 μm) was reached at 10 g/L talc. Further increase of the talc concentration did not result in a further reduction of the pellet size.

Taken together, smaller pellets were obviously beneficial for pamamycin production (Figure 3a). Microscopic analysis of the cultures revealed that the microparticles attached to the cells, which obviously loosened the inner structure of the aggregates (Figure 4c,d). The pellets of talc enhanced cultures appeared of a similar loose structure during growth and production phase. In contrast, the central core of pellets of the control culture showed signs of decomposition during production phase (Figure 4b).

3.4 | Microparticles globally reprogram the metabolism of *S. albus* J1074/R2

To assess the response of the actinomycete to the added microparticles in more detail, global gene expression analysis was conducted. We compared the transcriptome during the growth phase

(5 hr) and the production phase (21 hr) between a talc (10 g/L) supplied culture and a control culture without talc using RNA sequencing. Generally, the transition of *S. albus* J1074/R2 from the nonproducing growth phase to the production phase was linked to a wide readjustment of gene expression. The expression of 1,468 genes, representing 24% of the genomic repertoire, was significantly altered in the control culture, when cells shifted from growth to production mode (\log_2 -fold change ≥ 1 , $p \leq .05$; Figures S1 and S7). On top of this general shift, talc supply induced a global change in the transcriptome. These talc-specific effects were observed for the growth as well as the production phase (Figures 5, S1, and S6). Altogether, 3,341 genes (56% of all genes) were specifically affected by the presence of talc, revealing a fundamental impact of the microparticles on the physiology of *S. albus*. During growth, the microparticles changed the expression of 2,133 genes (36%). This number

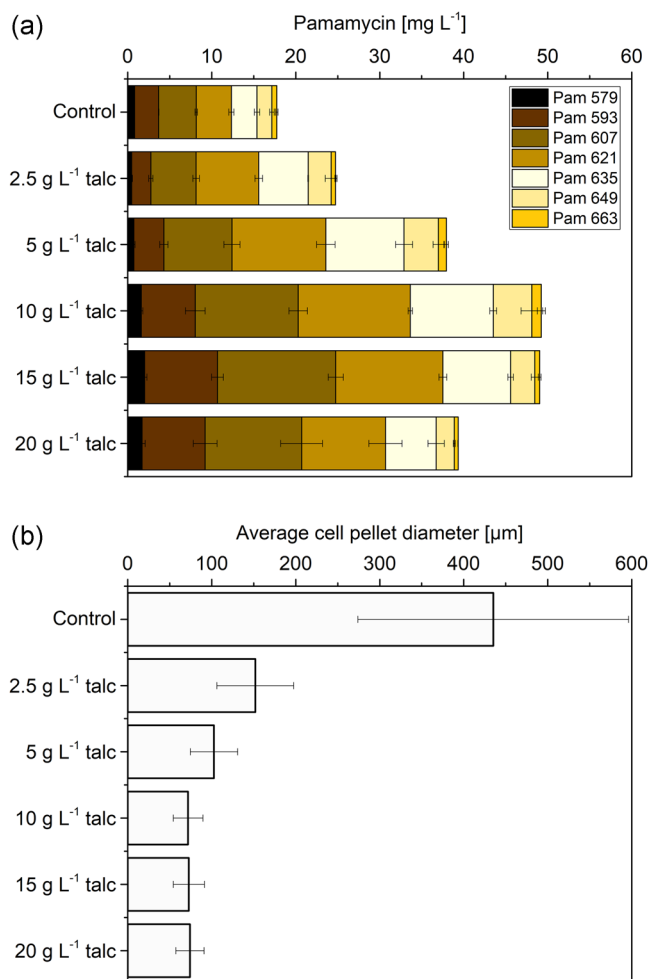


FIGURE 3 Streamlined pamamycin production using different concentrations of talc added to cultures of recombinant *Streptomyces albus* J1074/R2. (a) Total pamamycin titer and spectrum of different pamamycin derivatives assessed as final value after 48 hr of cultivation. (b) Average pellet diameter during the major production phase (20 hr), as assessed from optical analysis of at least 150 aggregates per condition [Color figure can be viewed at wileyonlinelibrary.com]

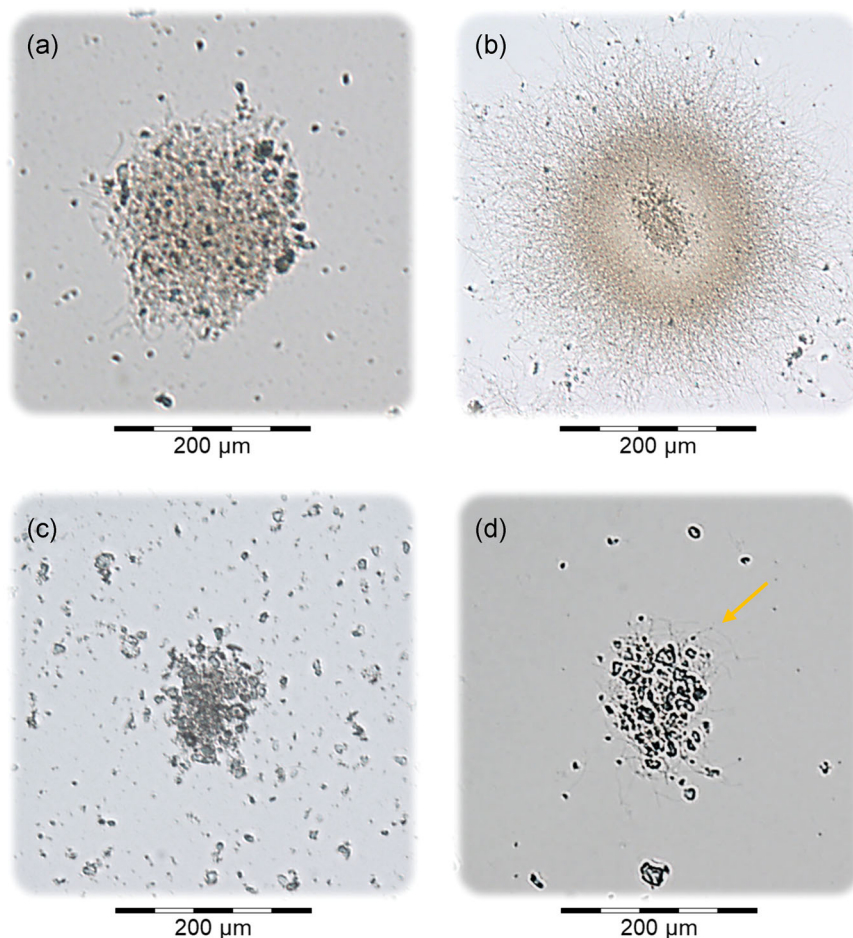


FIGURE 4 Impact of talc microparticles on the cellular morphology of *Streptomyces albus* J1074/R2. Control culture without microparticles during growth (5 hr) (a) and production (20 hr) (b). Microparticle-enhanced culture with 10 g/L talc during growth (5 hr) (c) and production (20 hr) (d). The arrow indicates the physical attachment of the mycelium to the microparticles [Color figure can be viewed at wileyonlinelibrary.com]

increased even further to 2,449 genes (41%), when talc supplemented cultures were in the production phase. The talc-induced changes covered almost all functional gene classes (Figure 5), which were found downregulated (shown in blue) or upregulated (yellow). As example, talc caused an upregulation of the biosynthetic pathways for branched chain amino acids, polyketide metabolism, and the biosynthesis of other secondary metabolites during the growth phase (Figure 5a). Talc specific gene expression changes during the production phase included an upregulation of starch and sucrose metabolism, valine, leucine and isoleucine degradation, butanoate metabolism, propanoate metabolism, fatty acid degradation, and secondary metabolite biosynthesis (Figure 5b). In addition, genes related to stress and cell death differed in transcription depending on culture conditions (Table S2).

3.5 | Talc microparticles affect the expression of morphology regulators

Since the microparticles obviously affected the morphology of *S. albus* (Figures 3b and 4), we searched within the transcriptome data for genes involved in morphology and secondary metabolism. Based on their similarity to known morphogenetic genes identified in other

Streptomyces, we could identify 55 genes which were affected by the particles (Figures S2 and S3). As prominent example, the addition of microparticles resulted in an upregulation (\log_2 -fold change = 2.0) of the sporulation and cell division protein SsgA, encoded by *XNRR2_5315*, already during growth (Table 1). The upregulation was even higher during production (\log_2 -fold change = 3.0). A similar picture was observed for other prominent morphology genes, that is, the signaling protein Factor C (*XNRR2_2306*), the chaplin (*chp*) and rodlin (*rdl*) hydrophobic sheath proteins and a neutral zinc metalloprotease (*XNRR2_1391*), a homolog to *sgmA* in *S. griseus*, and a well-known morphology regulator (Table 1). In all cases, the microparticles caused an overexpression, which was most pronounced during the pamamycin production phase but partly started already during growth.

3.6 | Microparticles drive the expression of the pamamycin biosynthetic cluster

Causally linked to the enhanced production, *S. albus* J1074/R2 responded to the microparticles by a strong overexpression of the pamamycin cluster (\log_2 -fold change up to 10, Figure 6). The activation was most pronounced for the production phase, where 19 out

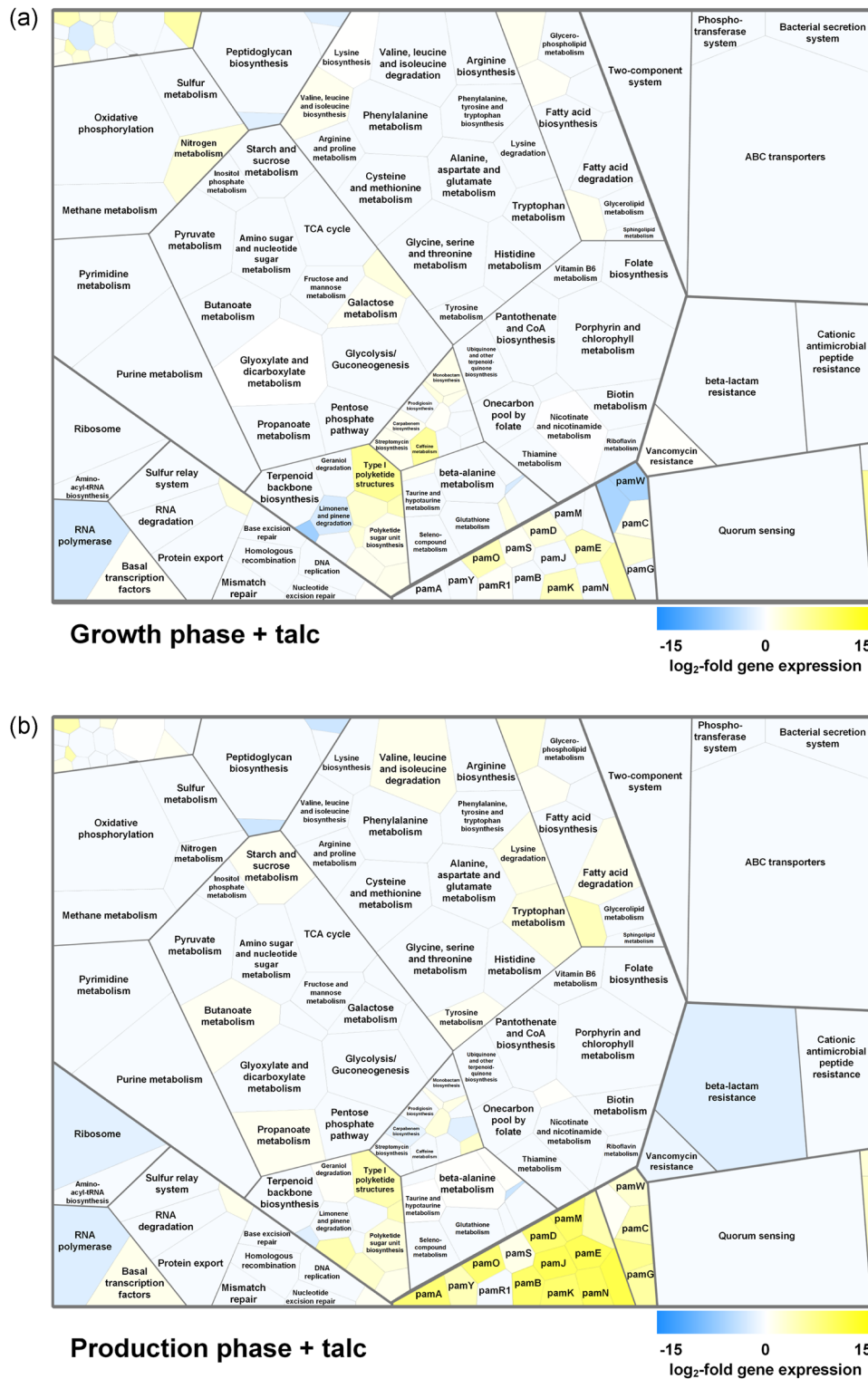


FIGURE 5 Global gene expression pattern for pamamycin producing *Streptomyces albus* J1074/R2 at different stages of the cultivation and under the impact of talc microparticles (10 g/L). Kyoto Encyclopedia of Genes and Genomes (KEGG)-orthology tree maps for the average gene expression of different functional classes of growing (a) and producing (b) *S. albus* J1074/R2 as compared to the control culture during as a reference. Each cell represents a functional class of the orthology: Carbohydrate metabolism, amino acid metabolism, lipid metabolism, nucleotide metabolism, energy metabolism, glycan biosynthesis and metabolism, xenobiotics biodegradation and metabolism, metabolism of cofactors and vitamins, metabolism of terpenoids and polyketides, biosynthesis of other secondary metabolites, metabolism of other amino acids, signal transduction, membrane transport, replication and repair, transcription, translation, folding, sorting and degradation, cellular community, and cell motility with their subclasses. The annotation was taken from the genome (entry T02545 in KEGG) of *S. albus* (Zaburannyi et al., 2014). In addition, the right and left core of the pamamycin gene cluster are shown [Color figure can be viewed at wileyonlinelibrary.com]

TABLE 1 Impact of talc microparticles on the expression of morphology associated genes in pamamycin producing *Streptomyces albus* J1074/R2

Gene	Annotation	Homolog and identity [%]	Growth (Talc)	Prod. (Talc)	Prod. (Control)	Reference
XNRR2_1044	Sporulation factor	<i>whiH</i> , SCO, 79.8	2.1	5.2	3.0	Flårdh, Kindlay, and Chater (1999)
XNRR2_1071	ppGpp synthetase	<i>relA</i> , SCO, 45.3	0.0	2.9	0.0	Hesketh et al. (2007)
XNRR2_5340	ppGpp synthetase I	<i>relA</i> , SCO, 85.6	0.0	0.0	0.0	Hesketh et al. (2007)
XNRR2_1554	Nucl. binding protein	<i>eshA</i> , SCO, 65.9	8.9	10.0	8.2	Saito et al. (2006)
XNRR2_1132	BldB	<i>bldB</i> , SALB	-1.0	-1.4	0.0	Flårdh et al. (1999)
XNRR2_1391	Metalloprotease	<i>sgmA</i> , SGR, 67.6	5.6	10.1	0.0	Kato, Suzuki, Yamazaki, Ohnishi, and Horinouchi (2002)
XNRR2_2151	Membrane protein	<i>chpD</i> , SALB	3.9	7.6	0.0	Zaburannyi et al. (2014)
XNRR2_2152	Secreted protein	<i>chpA</i> , SALB	0.0	7.0	0.0	Zaburannyi et al. (2014)
XNRR2_5022	Hypothetical protein	<i>chpE</i> , SALB	1.1	2.1	0.0	Zaburannyi et al. (2014)
XNRR2_5152	Membrane protein	<i>chpH</i> , SALB	3.3	8.1	4.3	Zaburannyi et al. (2014)
XNRR2_5153	Secreted protein	<i>chpC</i> , SALB	0.0	7.4	0.0	Zaburannyi et al. (2014)
XNRR2_2166	RdIB	<i>rdlB</i> , SALB	4.0	8.3	3.9	Claessen et al. (2004)
XNRR2_2167	RdIA	<i>rdlA</i> , SALB	5.2	10.5	4.1	Claessen et al. (2004)
XNRR2_2306	Factor C	<i>facC</i> , SALB	3.5	4.0	0.0	Birkó et al. (2007)
XNRR2_3527	BldN subunit	σ^{BldN} , SVE, 84.9	1.9	4.9	0.0	Bibb, Domonkos, Chandra, and Buttner (2012)
XNRR2_5117	TetR-type regulator	<i>wblA</i> , SCO, 67.8	4.2	4.5	4.2	van Wezel and McDowall (2011)
XNRR2_5315	SsgA	<i>ssgA</i> , SALB	2.0	3.0	1.8	van Wezel et al. (2000a)

Note: Samples were taken from a control and a talc supplied culture (10 g/L) in SGG medium during growth (5 hr) and production (21 hr). The values correspond to \log_2 -fold expression changes, considering the control culture during growth (5 hr) as reference. The listed genes represent previously discovered morphology-associated genes in *S. albus* (SALB) and genes, identified by BLAST search as homologs to morphology-associated genes in *S. coelicolor* (SCO), *S. griseus* (SGR), and *S. venezuelae* (SVE), indicated by the percentage of homology. The identification of homologs was supported by the fact that Streptomycetes share many genetic elements of morphology control (van Dissel et al., 2014), including SsgA like proteins (Traag & van Wezel, 2008) and Factor C (Birkó et al., 1999). In addition to genes identified in *S. albus* before (Zaburannyi, Rabyk, Ostash, Fedorenko, & Luzhetskyy, 2014), further candidates could be inferred from previous studies on morphological development in other *Streptomyces spp.*, including *S. coelicolor* (Chakraborty & Bibb, 1997; Hesketh et al., 2007; van Wezel & McDowall, 2011), *S. griseus* (Saito et al., 2006; van Wezel & McDowall, 2011), and *S. lividans* (van Wezel et al., 2006), among others.

of the 20 cluster genes were overexpressed as compared to the control. As exception, only the regulator gene *pamR1* remained relatively unaffected. It was interesting to note that the cluster activation was not fully balanced among the “two cores” of the gene cluster. In fact, genes of the “right core” were induced stronger than genes of the “left core.” Most of the “right core” genes, that is, 11 out of 15, were upregulated with a \log_2 -fold change of more than 8 by talc. A few genes of the pamamycin cluster (*pamC*, *pamD*, *pamE*, *pamF*, *pamH*, *pamK*, *pamO*, *pamS*, and *pamX*) were activated by the microparticles already during the growth phase. In contrast, the pamamycin transporter gene (*pamW*) and the regulator inside the “left core” (*pamR2*) were downregulated. In addition to the pamamycin cluster, also other genes of secondary metabolism were found significantly upregulated (Figure 5). The expression changes covered different gene functions: Type I polyketide structures (candicidin biosynthesis), polyketide sugar unit biosynthesis, siderophores (2,3-dihydroxybenzoate synthesis), sesquiterpenoid and triterpenoid

biosynthesis (germacradienol/geosmin synthase), terpenoid backbone synthesis, and phenazine biosynthesis (Table S3).

3.7 | Microparticles modulate supporting pathways in central carbon metabolism

As shown, cells preferably produced higher mass pamamycin derivatives in the presence of microparticles. Generally, different derivatives originate from the incorporation of different precursor metabolites, that is, CoA-esters of different type (Figure 1). We, therefore, hypothesized that the microparticles could have impacted genes encoding enzymes for CoA-ester synthesis and interconversion. Indeed, talc supply affected the expression of CoA-ester related genes (Table 2; Figures S4 and S5). As example, talc led to a strong downregulation (\log_2 -fold change = 6) of the α -subunit of the acetyl/propionyl-CoA carboxylase (XNRR2_4211), responsible for the formation of methylmalonyl-CoA

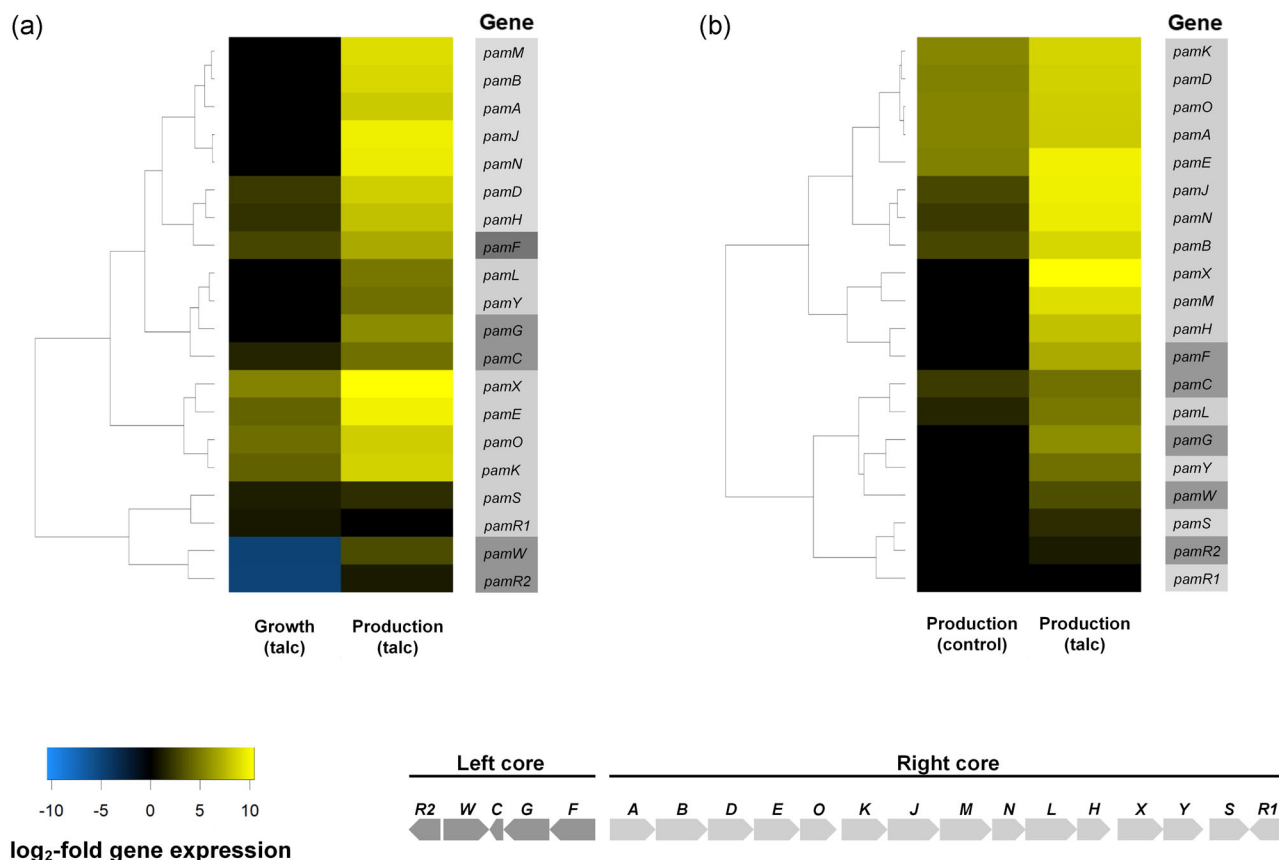


FIGURE 6 Hierarchical cluster analysis of the expression of the pamamycin biosynthetic pathway genes in *Streptomyces albus* J1074/R2. Samples were taken from a control and a talc supplied culture (10 g/L) in SGG medium during exponential growth (5 hr) and production phase (21 hr). The expression level of the control culture during growth (5 hr) was used as a reference. The cluster comprises the genes *pamA*, 3-oxoacyl-synthase 2; *pamB*, 3-oxoadipate CoA-transferase subunit A; *pamC*, acyl carrier protein; *pamD*, 3-oxoacyl-synthase 3 protein 1; *pamE*, 3-oxoacyl-synthase 3; *pamF*, 3-oxoacyl-synthase 2; *pamG*, 3-oxoacyl-synthase 3; *pamH*, aminohydrolase; *pamJ*, 3-oxoacyl-synthase 2; *pamK*, 3-oxoacyl-synthase 3; *pamL*, putative sulfoacetate-CoA ligase; *pamM*, 3-oxoacyl-reductase FabG; *pamN*, putative oxidoreductase; *pamO*, 3-oxoacyl-reductase FabG; *pamR1*, response regulator protein VraR; *pamR2*, tetracycline repressor protein class E; *pamS*, carnityl-CoA dehydratase; *pamW*, antiseptic resistance protein; *pamX*, L-lysine-8-amino-7-oxononanoate aminotransferase; *pamY*, cypemycin methyltransferase (Rebets et al., 2015) [Color figure can be viewed at wileyonlinelibrary.com]

from propionyl-CoA and the conversion of acetyl-CoA into malonyl-CoA. Moreover, talc supply resulted in the downregulation of methylmalonyl-CoA carboxyltransferase (*XNRR2_1278*). In contrast, elevated expression of acetyl-CoA acetyltransferase (*XNRR2_0301*, *XNRR2_1438*, *XNRR2_1987*), acetoacetyl-CoA synthetase (*XNRR2_5448*) crotonyl-CoA carboxylase/reductase (*XNRR2_0456*, *XNRR2_5889*), methylmalonyl-CoA mutase (*XNRR2_4665*, *XNRR2_4666*), and methylmalonyl-CoA epimerase (*XNRR2_1439*) was observed (Table 2).

3.8 | Microparticles affect intracellular CoA-ester pools during pamamycin production in *S. albus* J1074/R2

Due to the significant transcriptomic changes around the pamamycin cluster and the genes of its precursor metabolism, it

appeared interesting to assess the availability of the product precursors during the production process. We focused our analysis on 11 CoA-esters that are either directly incorporated into pamamycins, that is, succinyl-CoA, malonyl-CoA, methylmalonyl-CoA, and ethylmalonyl-CoA (Figure 1), or are connected to these building blocks. For this purpose, we acquired CoA-ester levels in a talc supplied (10 g/L) and a control culture during the major phase of production (20 hr). Interestingly, the microparticles strongly affected the CoA-ester pools (Figure 7). The level of malonyl-CoA (-48%), methylsuccinyl-CoA (-46%), crotonyl-CoA (-32%), and acetyl-CoA (-19%) was strongly decreased. In contrast, the pool of methylmalonyl-CoA was increased by more than 100%. Furthermore, the microparticles increased the level of acetoacetyl-CoA (+250%) and the pool of the isomers butyryl-/isobutyryl-CoA (+169%). The abundance of succinyl-CoA, propionyl-CoA, and ethylmalonyl-CoA remained unchanged.

Gene	Annotation	Growth (Talc)	Prod. (Talc)	Prod. (Control)
XNRR2_0221	Enoyl-CoA hydratase	0.0	5.0	0.0
XNRR2_0301	Acetyl-CoA acetyltransferase	0.0	4.3	0.0
XNRR2_0454	3-Hydroxybutyryl-CoA dehydrogenase	3.2	-1.0	0.0
XNRR2_0456	Crotonyl-CoA carboxylase/reductase	11.3	3.8	0.0
XNRR2_0457	Ethylmalonyl-CoA mutase	8.5	0.0	0.0
XNRR2_1278	Methylmalonyl-CoA decarboxylase	-3.2	-2.3	0.0
XNRR2_1304	Branched-chain amino acid aminotransferase	2.0	1.5	0.0
XNRR2_1417	Isobutyryl-CoA mutase	-1.0	1.3	0.0
XNRR2_1438	Acetyl-CoA acetyltransferase	2.9	4.3	0.0
XNRR2_1439	Methylmalonyl-CoA epimerase; ethylmalonyl-CoA epimerase	3.3	2.3	0.0
XNRR2_1452	3-Hydroxybutyryl-CoA dehydrogenase	1.0	1.3	0.0
XNRR2_1987	Acetyl-CoA acetyltransferase	3.3	3.7	0.0
XNRR2_2839	Valine dehydrogenase	1.1	2.2	0.0
XNRR2_3056	Branched-chain alpha-keto acid dehydrogenase E2	-1.7	0.0	0.0
XNRR2_3069	Branched-chain alpha-keto acid dehydrogenase E2	1.4	0.0	0.0
XNRR2_3858	Isobutyryl CoA mutase, small subunit	1.9	1.8	0.0
XNRR2_4024	Propionyl-CoA carboxylase, beta subunit	2.2	1.2	1.0
XNRR2_4211	Acetyl-/propionyl-CoA carboxylase α -subunit	-6.0	1.7	0.0
XNRR2_4665	Methylmalonyl-CoA mutase large subunit	1.6	2.2	0.0
XNRR2_4666	Methylmalonyl-CoA small subunit	2.2	2.3	0.0
XNRR2_5448	Acetoacetyl-CoA synthetase	8.0	5.9	0.0
XNRR2_5889	Crotonyl-CoA reductase	9.0	8.2	8.6

Note: Samples were taken from a control and a talc supplied culture (10 g/L) in SGG medium during growth (5 hr) and production (21 hr). The values correspond to \log_2 -fold expression changes, considering the control during growth (5 hr) as reference. The annotation was taken from the genome (entry T02545 in KEGG) of *S. albus* (Zaburannyi et al., 2014).

4 | DISCUSSION

4.1 | Microparticle-enhanced production supports future exploration of pamamycins as lead molecules for novel antituberculosis drugs

As shown in this study, talc microparticles increased the production of pamamycins in recombinant *S. albus* J1074/R2 almost threefold to 50 mg/L, the highest titer observed so far for these polyketides (Figure 3). In this regard, the strongly improved pamamycin production by addition of talc is supposed to facilitate

TABLE 2 Impact of talc microparticles on the expression of genes associated to CoA-thioester metabolism in pamamycin producing *Streptomyces albus* J1074/R2

future exploration of this important polyketide. As shown, only small amounts of talc were required to achieve the stimulating effect (Figures 2 and 3), so that a use of this cheap material for pamamycin production appears feasible also from a cost perspective. Remarkably, the addition of talc selectively triggered the formation of larger variants (Figure 3a), that is, Pam 635, Pam 649, and Pam 663. Due to the fact that the different derivatives apparently differ in biological activity (Lefèvre et al., 2004; Natsume, 2016), a microparticle-based process might help to selectively enrich heavier pamamycin variants in the total product spectrum with potentially other activities.

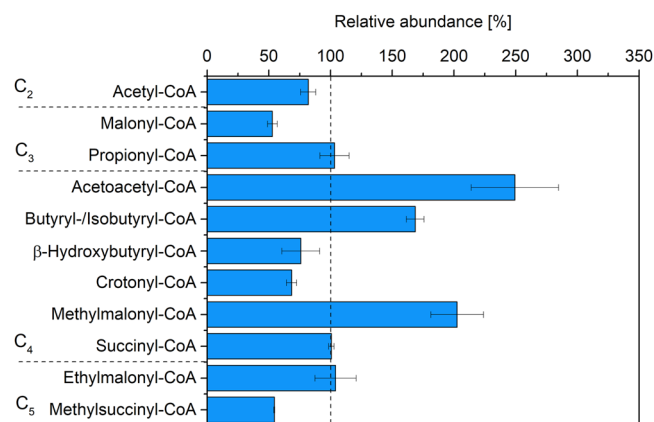


FIGURE 7 Relative changes of intracellular CoA-ester pools in pamamycin producing *Streptomyces albus* J1074/R2 by the addition of talc microparticles (10 g/L) to the culture during the major production phase (21 hr). The intracellular availability of 11 CoA-esters, directly and indirectly linked to pamamycin assembly was assessed during the production phase (21 hr) of a talc supplied and a control culture (set to 100%, shown as dashed line) [Color figure can be viewed at wileyonlinelibrary.com]

4.2 | Pamamycin production in *S. albus* is linked to morphological development

The obtained RNA sequencing data provided a detailed insight into the dynamics of morphology development along the production process (Figures 5, 6, and S1–S7; Tables 1 and 2). As shown for the control, genes encoding morphology regulators and morphogenetic proteins were strongly activated during the shift from growth to production (Figure 8). These comprised prominent players of morphology control in Streptomyces: (a) *XNRR2_1071* (RelA) providing ppGpp, known to control morphogenetic proteins (Hesketh, Chen, Ryding, Chang, & Bibb, 2007), (b) *XNRR2_1554* (EshA) supporting ppGpp accumulation and essential for morphology development in *S. griseus* (Saito et al., 2006; van Wezel & McDowall, 2011); (c) *XNRR2_5315* (SsgA), limiting hyphae growth and branching, supporting septation, and formation of spore-like compartments (van Wezel, van der Meulen, Taal, Koerten, & Kraal, 2000b); (d) *XNRR2_2306* (Factor C protein), stimulating sporulation in submerged culture (Birkó et al., 1999; van Wezel & McDowall, 2011); (e) hydrophobic coat proteins such as chaplins and rodlines, which form the surface rodlet layer on spores (Claessen et al., 2004); and (f) *XNRR2_3527* (sigma factor BldN) controlling their expression in *S. venezuelae* (Bibb et al., 2012) and likely in *S. coelicolor* (McCormick & Flärdh, 2012; Figure 8; Table 1). There seems no doubt that this morphological development during the culture triggered the pamamycin formation (van Wezel & McDowall, 2011). It was interesting to note that the addition of talc influenced the utilization of nutrients, including phosphate and glycerol (Figure S8) and furthermore affected the amount of biomass formed (Figure 2). We cannot provide a clear conclusion

on the underlying effects at this point but would like to notice that the understanding of these effects remains an important question.

4.3 | Microparticles accelerate the morphogenesis of *S. albus* toward sporulation-oriented mycelial development and cell division

Notably, the morphogenesis program was massively upregulated in the presence of the talc particles (Figure 8; Table 1). The activation was already visible during the initial growth phase and was even stronger during the later production phase. It was observed for practically all genes, which were identified as part of the morphology control cascade. We therefore conclude that the microparticles significantly speeded up the aging of the *S. albus* culture and accelerated the shift to second mycelium formation and submerged sporulation response. It appears highly likely that the enhanced pamamycin formation, including a strong overexpression of the *pam* cluster itself, was a consequence of the accelerated morphogenesis program, induced by the microparticles. It is well known that natural product formation is linked to morphological differentiation in Streptomyces (Chater, 1984), so that its perturbation can be efficiently exploited to influence antibiotic production in *S. coelicolor*, *S. lividans*, and other species (Chakraborty & Bibb, 1997; Hesketh et al., 2007; van Wezel & McDowall, 2011). Admittedly, the data did not allow to identify the specific link between morphology development, pamamycin cluster expression, and altered expression of its two regulators (Figure 6). More work will be needed in the future to resolve this in greater detail. *S. albus* possesses a range of different (mainly uncharacterized) ECF sigma factors and regulators, of which the majority was found affected by talc and gives a flavor of the complexity to be explored (Table S1).

4.4 | Talc microparticles orchestrate the regulatory and metabolic network of *S. albus* to a highly efficient program for pamamycin production

We now mapped the obtained transcriptomic and metabolomic data on the carbon core network of *S. albus* to obtain a systems-view on pamamycin production and supporting pathways (Figure 9). First, specific adjustments were observed in central carbon metabolism. Genes, related to conversion of glycerol were generally upregulated during the major production phase, linked to the on-set of glycerol consumption at this point (Figure S8). This substrate shift could also explain the increased expression of the EMP pathway genes alongside the downregulation of the oxidative PP pathway at the level of 6-phosphogluconate dehydrogenase. The effects were slightly more pronounced in the presence of talc. Second, most genes encoding for enzymes of CoA-ester metabolism were upregulated by the microparticles as

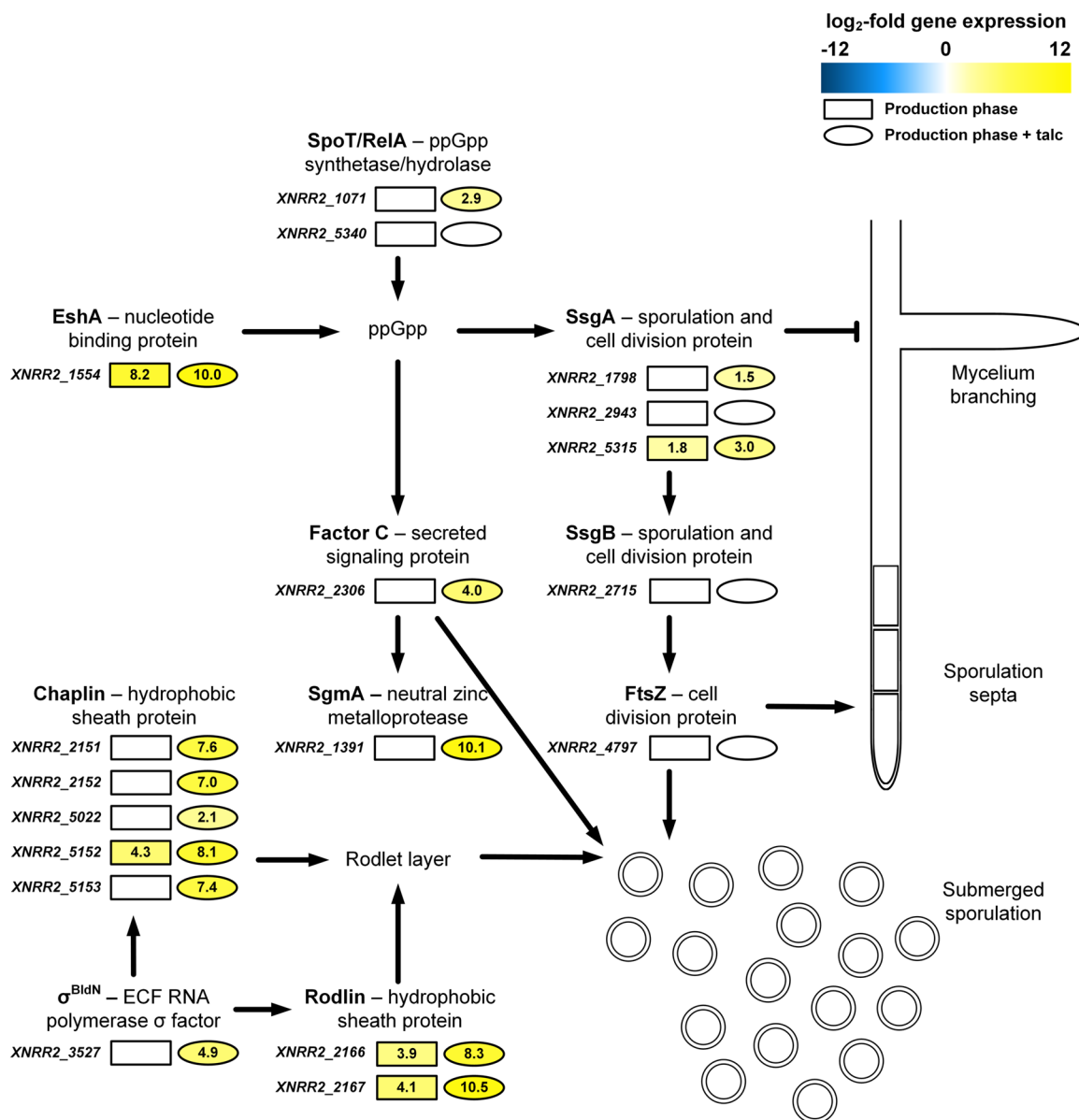


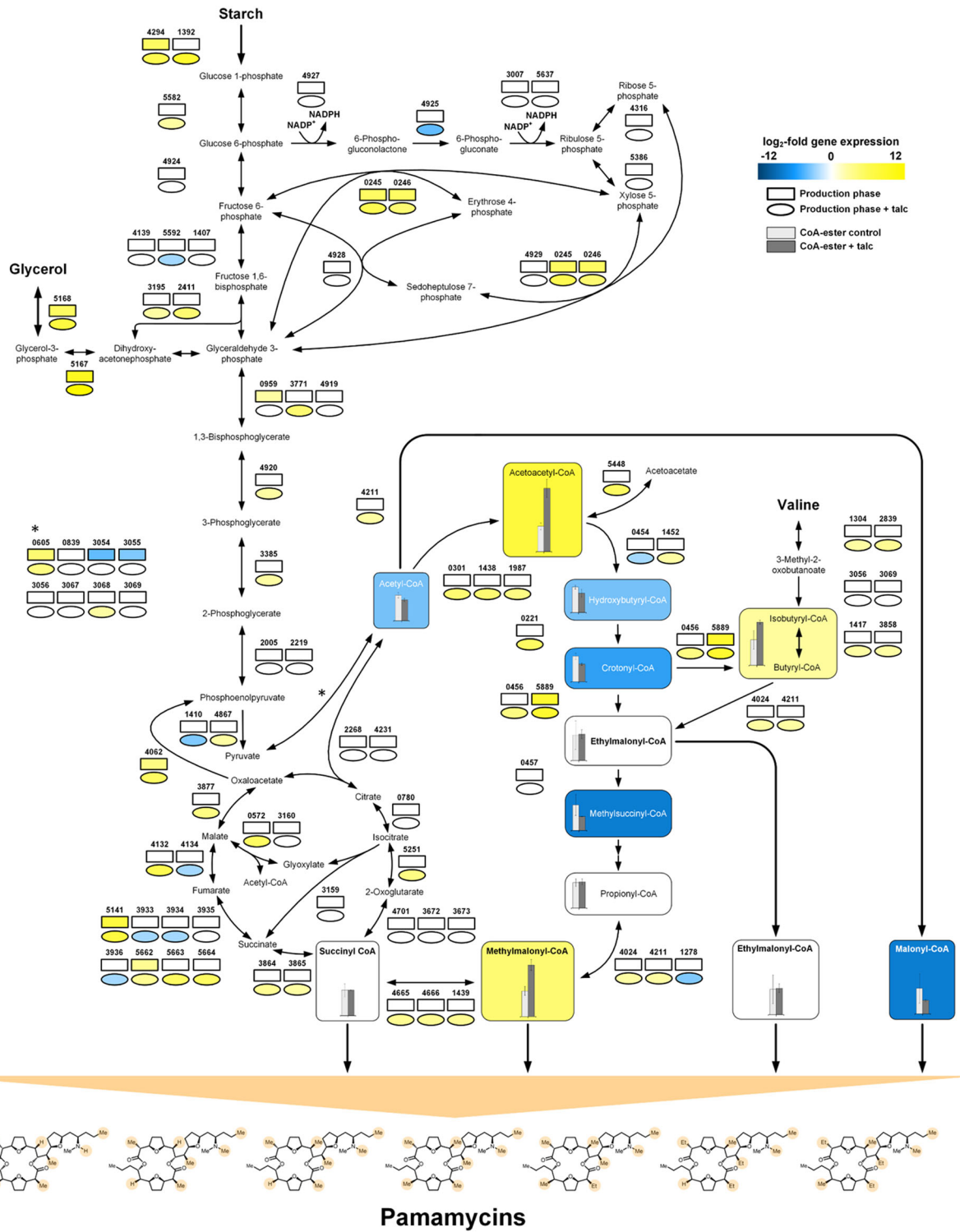
FIGURE 8 Impact of talc microparticles on the morphogenesis of pamamycin producing *Streptomyces albus* J1074/R2 in submerged culture. The data reflect differential gene expression of morphology-associated genes during the pamamycin production phase (21) in the presence of 10 g/L talc (ellipse) and the control process without particles (rectangle). The gene expression during the growth phase (5 hr) of the control is used as a reference. The numbers denote log₂-fold expression change. Further details on the displayed components of the morphology cascade are given in Table 2 [Color figure can be viewed at wileyonlinelibrary.com]

well and resulted in a modulation of CoA-ester availability. Third, the changes in the CoA-ester metabolism had direct impact on the spectrum of pamamycins formed. It was interesting to note that the particles perturbed the ratio between malonyl-CoA, methylmalonyl-CoA, and ethylmalonyl-CoA (Figure 7). The three building blocks compete for incorporation into pamamycin. The polyketide assembly line equally accepts them as substrates, which leads to 16 pamamycin derivatives that differ in their side chains at six positions (Rebets et al., 2015). As shown, microparticle-affected cells produced more than twofold less small pamamycins (Pam 579 and Pam 593), whereas heavier

derivatives were enriched (Pam 607, Pam 621, Pam 635, Pam 649, and Pam 663).

We conclude that this was the consequence of an increased availability of the larger building block methylmalonyl-CoA, together with a reduction in the malonyl-CoA pool.

It would be interesting to further explore this link in other natural producers, which obviously differ in the spectrum of pamamycin homologues (Natsume, Yasui, Kondo, & Marumo, 1991; Natsume et al., 1995; Kozone, Chikamoto, Abe, & Natsume, 1999). Metabolic engineering of CoA-ester supply appears promising to streamline pamamycin production towards selective derivatives (Lu, Zhang, Jiang, & Bai, 2016).



5 | CONCLUSIONS

We could show that talc microparticles globally reprogrammed the metabolism of *S. albus*, forced an accelerated morphological development, and triggered expression of the pamamycin cluster and supporting pathways. Despite the long tradition and the great success microparticles as process agents for filamentous microbes, it has remained largely unclear how the particles actually mediate the observed effects on the molecular level (Antecka, Bizukojc, & Ledakowicz, 2016). In this regard, our insights appear of general value for further exploration and industrialization of microparticle-enhanced processes. The use of microparticles, furthermore promises to support strain engineering by suggesting novel genetic targets, given the rich response on the genomic level observed in this study. Altogether, it appears fair to state that microparticle-enhanced production is advancing into a broadly applicable strategy to tailor *Streptomyces*, *Amycolatopsis*, and other related filamentous Actinomycetes for natural product formation (e.g. rifamycin, ivermectin, etc.) and should be further explored to support their discovery, development, and industrialization (Barton et al., 2018). During the work, the streamlined *S. albus* "clean" chassis turned out to grow fast and exhibit high and stable pamamycin biosynthesis, suggesting further use (Myronovskiy et al., 2018). "Cluster-free" chassis strains appear particularly promising for selective production in the future, given the activation of native clusters observed here (Figure 5).

ACKNOWLEDGMENTS

The work of Martin Kuhl, Lars Gläser, and Christoph Wittmann was supported by the German Ministry of Education and Research (BMBF) under Grant MyBio (FKZ 031B0344A) and the German Research Foundation (FKZ INST 256/418-1). The work of Yuri Rebets and Andriy Luzhetskyy was supported by the BMBF under Grant MyBio (FKZ 031B0344B). The work of Christian Rückert and Jörn Kalinowski acknowledge funding by the BMBF through the grant MyBio (FKZ 031B0344C). Thomas Hartsch and Namrata Sarkar was supported by the BMBF under Grant MyBio (FKZ 031B0344D). The funding bodies did not contribute to study design, data collection, analysis, and interpretation, or writing of the manuscript. Open access funding enabled and organized by Projekt DEAL.

CONFLICT OF INTERESTS

Yuriy Rebets and Andriy Luzhetskyy have submitted a patent application to produce pamamycin in *S. albus*. The other authors declare that there are no conflict of interests.

AUTHOR CONTRIBUTIONS

C. W. designed the project. M. K. conducted the cultures. M. K. and Y. R. performed pamamycin analysis. M. K. and L. G. performed CoA ester analysis. C. R. and J. K. performed RNA sequencing. C. R., J. K., N. S., and T. H. processed and evaluated the RNA sequencing data. M. K. and C. W. analyzed the data, drew the figures, and wrote the first draft of the manuscript. All authors commented, extended, and improved the manuscript. All authors read and approved the final version of the manuscript.

DATA AVAILABILITY STATEMENT

The raw and processed RNA sequencing data of this article are available as MIAME-compliant datasets in Gene Expression Omnibus under the accession number GSE155008. The authors declare that all other data supporting the findings of this study are available within the article and its supplementary information file.

ORCID

Jörn Kalinowski  <https://orcid.org/0000-0002-9052-1998>

Andriy Luzhetskyy  <https://orcid.org/0000-0001-6497-0047>

Christoph Wittmann  <http://orcid.org/0000-0002-7952-985X>

REFERENCES

- Ahmed, Y., Rebets, Y., Estevez, M. R., Zapp, J., Myronovskiy, M., & Luzhetskyy, A. (2020). Engineering of *Streptomyces lividans* for heterologous expression of secondary metabolite gene clusters. *Microbial Cell Factories*, 19(1), 5. <https://doi.org/10.1186/s12934-020-1277-8>
- Angert, E. R. (2005). Alternatives to binary fission in bacteria. *Nature Reviews Microbiology*, 3(3), 214–224. <https://doi.org/10.1038/nrmicro1096>
- Antecka, A., Bizukojc, M., & Ledakowicz, S. (2016). Modern morphological engineering techniques for improving productivity of filamentous fungi in submerged cultures. *World Journal of Microbiology & Biotechnology*, 32(12), 193. <https://doi.org/10.1007/s11274-016-2148-7>

FIGURE 9 Multiomics view on the effect of talc microparticles on pathways supporting pamamycin biosynthesis in *Streptomyces albus* J1074/R2 during the production phase. The boxes indicate differential gene expression of the control (rectangle) and the talc supplied process (10 g/L talc, ellipse) during the major production phase, as compared to the reference (control in growth phase, boxes indicate XNRR2 numbers). The bar charts display relative CoA-ester availability. Although CCR (XNRR2_0456 and XNRR2_5889) and PCC (XNRR2_4024 and XNRR2_4211) might be able to convert crotonyl-CoA to butyryl-CoA and butyryl-CoA to ethylmalonyl-CoA, respectively, their main activity catalyzes the formation of ethylmalonyl-CoA and propionyl-CoA, respectively (Chan, Podevels, Kevany, & Thomas, 2009). The observed changes in CoA ester metabolism were complex. Direct correlations between one particular thioester and one enzyme appeared infeasible, due to this complexity and the known promiscuity of several of the CoA-ester converting enzymes (Chan et al., 2009). However, a few conclusions could be drawn. The genes, encoding for reactions upstream of increased CoA-ester pools, that is, acetoacetyl-CoA, (iso)butyryl-CoA, and methylmalonyl-CoA were found upregulated, which suggests that the accumulation was related to an enhanced biosynthesis. In addition, the entry steps into the CoA metabolism were found massively altered. The flux from acetyl-CoA was largely redirected to form acetoacetyl-CoA, instead of malonyl-CoA. The data further suggested that the increased amount of methylmalonyl CoA was mainly derived from succinyl-CoA. The alternative ethylmalonyl CoA route appeared attenuated because major intermediates involved, that is, hydroxybutyryl-CoA, crotonyl-CoA, methylsuccinyl-CoA, were found reduced [Color figure can be viewed at wileyonlinelibrary.com]

- Arcamone, F., Cassinelli, G., Fantini, G., Grein, A., Orezzi, P., Pol, C., & Spalla, C. (1969). Adriamycin, 14-hydroxydaimomycin, a new antitumor antibiotic from *S. Peuceius* var. *caesius*. *Biotechnology and Bioengineering*, 11(6), 1101–1110. <https://doi.org/10.1002/bit.260110607>
- Barton, N., Horbal, L., Starck, S., Kohlstedt, M., Luzhetskyy, A., & Wittmann, C. (2018). Enabling the valorization of guaiacol-based lignin: Integrated chemical and biochemical production of cis, cis-muonic acid using metabolically engineered *Amycolatopsis* sp ATCC 39116. *Metabolic Engineering*, 45, 200–210. <https://doi.org/10.1016/j.mbs.2017.12.001>
- Bayer, E., Gugel, K., Hägele, K., Hagenmaier, H., Jessipow, S., König, W., & Zähler, H. (1972). Stoffwechselprodukte von Mikroorganismen. 98. Mitteilung. Phosphinothricin und Phosphinothricin-Alanyl-Alanin. *Helvetica Chimica Acta*, 55(1), 224–239. <https://doi.org/10.1002/hlca.19720550126>
- Becker, J., Klopprogge, C., Schröder, H., & Wittmann, C. (2009). Metabolic engineering of the tricarboxylic acid cycle for improved lysine production by *Corynebacterium glutamicum*. *Applied and Environmental Microbiology*, 75(24), 7866–7869. <https://doi.org/10.1128/AEM.01942-09>
- Belmar-Beiny, M., & Thomas, C. (1991). Morphology and clavulanic acid production of *Streptomyces clavuligerus*: Effect of stirrer speed in batch fermentations. *Biotechnology and Bioengineering*, 37(5), 456–462. <https://doi.org/10.1002/bit.260370507>
- Bibb, M. J. (2013). Understanding and manipulating antibiotic production in Actinomycetes. *Biochemical Society Transactions*, 41(6), 1355–1364. <https://doi.org/10.1042/BST20130214>
- Bibb, M. J., Domonkos, Á., Chandra, G., & Buttner, M. J. (2012). Expression of the chaplin and rodlin hydrophobic sheath proteins in *Streptomyces venezuelae* is controlled by σ BldN and a cognate anti-sigma factor, RsbN. *Molecular Microbiology*, 84(6), 1033–1049. <https://doi.org/10.1111/j.1365-2958.2012.08070.x>
- Birkó, Z., Bialek, S., Buzás, K., Szajli, E., Traag, B. A., Medzihradzky, K. F., ... Biró, S. (2007). The secreted signaling protein factor C triggers the A-factor response regulon in *Streptomyces griseus*: Overlapping signaling routes. *Molecular & Cellular Proteomics*, 6(7), 1248–1256. <https://doi.org/10.1074/mcp.M600367-MCP200>
- Birkó, Z., Sümegi, A., Vinnai, A., Van Wezel, G., Szeszák, F., Vitális, S., ... Biró, S. (1999). Characterization of the gene for factor C, an extracellular signal protein involved in morphological differentiation of *Streptomyces griseus*. *Microbiology*, 145(9), 2245–2253. <https://doi.org/10.1099/00221287-145-9-2245>
- Campbell, W. C., Fisher, M. H., Stapley, E. O., Albers-Schönberg, G., & Jacob, T. A. (1983). Ivermectin: A potent new antiparasitic agent. *Science*, 221(4613), 823–828. <https://doi.org/10.1126/science.6308762>
- Chakraborty, R., & Bibb, M. (1997). The ppGpp synthetase gene (*relA*) of *Streptomyces coelicolor* A3 (2) plays a conditional role in antibiotic production and morphological differentiation. *Journal of Bacteriology*, 179(18), 5854–5861. <https://doi.org/10.1128/jb.179.18.5854-5861.1997>
- Chan, Y. A., Podevels, A. M., Kevany, B. M., & Thomas, M. G. (2009). Biosynthesis of polyketide synthase extender units. *Natural Product Reports*, 26(1), 90–114. <https://doi.org/10.1039/b801658p>
- Chater, K. F. (1984). Morphological and physiological differentiation in *Streptomyces*. *Microbial Development*, 16, 89–115. <https://doi.org/10.1101/0.89-115>
- Chater, K. F., & Losick, R. (1997). Mycelial life style of *Streptomyces coelicolor* A3 (2) and its relatives, *Multicellular and interactive behavior of bacteria: In nature, industry and the laboratory* (pp. 149–182). Oxford, UK: Oxford University Press.
- Claessen, D., Stokroos, I., Deelstra, H. J., Penninga, N. A., Bormann, C., Salas, J. A., ... Wösten, H. A. (2004). The formation of the rodlet layer of *Streptomyces* is the result of the interplay between rodlines and chaplins. *Molecular Microbiology*, 53(2), 433–443. <https://doi.org/10.1111/j.1365-2958.2004.04143.x>
- van Dissel, D., Claessen, D., & van Wezel, G. P. (2014). Morphogenesis of *Streptomyces* in submerged cultures, *Advances in Applied Microbiology* (89, pp. 1–45). Amsterdam, The Netherlands: Elsevier.
- Driouch, H., Hänsch, R., Wucherpfennig, T., Krull, R., & Wittmann, C. (2012). Improved enzyme production by bio-pellets of *Aspergillus niger*: Targeted morphology engineering using titanate microparticles. *Biotechnology and Bioengineering*, 109(2), 462–471. <https://doi.org/10.1002/bit.23313>
- Driouch, H., Roth, A., Dersch, P., & Wittmann, C. (2010). Filamentous fungi in good shape: Microparticles for tailor-made fungal morphology and enhanced enzyme production. *Bioengineered Bugs*, 2(2), 100–104. <https://doi.org/10.4161/bbug.2.2.13757>
- Driouch, H., Sommer, B., & Wittmann, C. (2010). Morphology engineering of *Aspergillus niger* for improved enzyme production. *Biotechnology and Bioengineering*, 105(6), 1058–1068. <https://doi.org/10.1002/bit.22614>
- Ehrlich, J., Bartz, Q. R., Smith, R. M., Joslyn, D. A., & Burkholder, P. R. (1947). Chloromycetin, a new antibiotic from a soil actinomycete. *Science*, 106(2757), 417. <https://doi.org/10.1126/science.106.2757.417>
- Etschmann, M. M., Huth, I., Walisko, R., Schuster, J., Krull, R., Holtmann, D., ... Schrader, J. (2015). Improving 2-phenylethanol and 6-pentyl- α -pyrone production with fungi by microparticle-enhanced cultivation (MPEC). *Yeast*, 32(1), 145–157. <https://doi.org/10.1002/yea.3022>
- Flärdh, K., Kindlay, K. C., & Chater, K. F. (1999). Association of early sporulation genes with suggested developmental decision points in *Streptomyces coelicolor* A3(2). *Microbiology*, 145(9), 2229–2243.
- Glazebrook, M. A., Vining, L. C., & White, R. L. (1992). Growth morphology of *Streptomyces akiyoshiensis* in submerged culture: Influence of pH, inoculum, and nutrients. *Canadian Journal of Microbiology*, 38(2), 98–103. <https://doi.org/10.1139/m92-016>
- Gläser, L., Kuhl, M., Jovanovic, S., Fritz, M., Vögeli, B., Erb, T., ... Wittmann, C. (2020). A common approach for absolute quantification of short chain CoA thioesters in industrially relevant gram-positive and gram-negative prokaryotic and eukaryotic microbes. *Microbial Cell Factories*, 19, 160.
- Hanquet, G., Salom-Roig, X., & Lanners, S. (2016). New insights into the synthesis and biological activity of the pamamycin macrodiolides. *Chimia*, 70(1-2), 20–28. <https://doi.org/10.2533/chimia.2016.20>
- Hesketh, A., Chen, W. J., Ryding, J., Chang, S., & Bibb, M. (2007). The global role of ppGpp synthesis in morphological differentiation and antibiotic production in *Streptomyces coelicolor* A3 (2). *Genome Biology*, 8(8), R161. <https://doi.org/10.1186/gb-2007-8-8-r161>
- Hilker, R., Stadermann, K. B., Doppmeier, D., Kalinowski, J., Stoye, J., Straube, J., ... Goesmann, A. (2014). ReadXplorer—visualization and analysis of mapped sequences. *Bioinformatics*, 30(16), 2247–2254. <https://doi.org/10.1093/bioinformatics/btu205>
- Holtmann, D., Vernen, F., Müller, J., Kaden, D., Risse, J. M., Friehs, K., ... Schrader, J. (2017). Effects of particle addition to *Streptomyces* cultivations to optimize the production of actinorhodin and streptavidin. *Sustainable Chemistry and Pharmacy*, 5, 67–71. <https://doi.org/10.1016/j.scp.2016.09.001>
- Horbal, L., Marques, F., Nadmid, S., Mendes, M. V., & Luzhetskyy, A. (2018). Secondary metabolites overproduction through transcriptional gene cluster refactoring. *Metabolic Engineering*, 49, 299–315. <https://doi.org/10.1016/j.mbs.2018.09.010>
- Jonsbu, E., McIntyre, M., & Nielsen, J. (2002). The influence of carbon sources and morphology on nystatin production by *Streptomyces noursei*. *Journal of Biotechnology*, 95(2), 133–144. [https://doi.org/10.1016/s0168-1656\(02\)00003-2](https://doi.org/10.1016/s0168-1656(02)00003-2)
- Juarez, M., Schcolnik-Cabrera, A., & Dueñas-Gonzalez, A. (2018). The multitargeted drug ivermectin: From an antiparasitic agent to a repositioned cancer drug. *American Journal of Cancer Research*, 8(2), 317–331.
- Kallifidas, D., Jiang, G., Ding, Y., & Luesch, H. (2018). Rational engineering of *Streptomyces albus* J1074 for the overexpression of secondary metabolite gene clusters. *Microbial Cell Factories*, 17(1), 25. <https://doi.org/10.1186/s12934-018-0874-2>
- Kato, J.-y., Suzuki, A., Yamazaki, H., Ohnishi, Y., & Horinouchi, S. (2002). Control by A-factor of a metalloendopeptidase gene involved in aerial mycelium formation in *Streptomyces griseus*.

- Journal of Bacteriology*, 184(21), 6016–6025. <https://doi.org/10.1128/JB.184.21.6016-6025.2002>
- Kaup, B. A., Ehrich, K., Pescheck, M., & Schrader, J. (2008). Microparticle-enhanced cultivation of filamentous microorganisms: Increased chloroperoxidase formation by *Caldariomyces fumago* as an example. *Biotechnology and Bioengineering*, 99(3), 491–498. <https://doi.org/10.1002/bit.21713>
- Kieser, T., Bibb, M. J., Buttner, M. J., Chater, K. F., & Hopwood, D. A. (2000). An introduction to *Streptomyces*. *Practical Streptomyces genetics* (p. 291). Norwich, UK: John Innes Foundation.
- Koebisch, I., Overbeck, J., Piepmeyer, S., Meschke, H., & Schrempf, H. (2009). A molecular key for building hyphae aggregates: The role of the newly identified *Streptomyces* protein HyaS. *Microbial Biotechnology*, 2(3), 343–360. <https://doi.org/10.1111/j.1751-7915.2009.00093.x>
- Kozone, I., Chikamoto, N., Abe, H., & Natsume, M. (1999). De-N-methylpamamycin-593A and B, new pamamycin derivatives isolated from *Streptomyces alboniger*. *Journal of Antibiotics*, 52(3), 329–331. <https://doi.org/10.7164/antibiotics.52.329>
- Krull, R., Wucherpfennig, T., Esfandabadi, M. E., Walisko, R., Melzer, G., Hempel, D. C., ... Wittmann, C. (2013). Characterization and control of fungal morphology for improved production performance in biotechnology. *Journal of Biotechnology*, 163(2), 112–123. <https://doi.org/10.1016/j.jbiotec.2012.06.024>
- Langmead, B., & Salzberg, S. L. (2012). Fast gapped-read alignment with Bowtie 2. *Nature Methods*, 9(4), 357–359. <https://doi.org/10.1038/nmeth.1923>
- Lechevalier, H., Acker, R. F., Corke, C. T., Haenseler, C. M., & Waksman, S. A. (1953). Candicidin, a new antifungal antibiotic. *Mycologia*, 45(2), 155–171. <https://doi.org/10.1080/00275514.1953.12024259>
- Lefèvre, P., Peirs, P., Braibant, M., Fauville-Dufaux, M., Vanhoof, R., Huygen, K., ... Content, J. (2004). Antimycobacterial activity of synthetic pamamycins. *Journal of Antimicrobial Chemotherapy*, 54(4), 824–827. <https://doi.org/10.1093/jac/dkh402>
- Liu, X., Tang, J., Wang, L., & Liu, R. (2019). Mechanism of CuO nanoparticles on stimulating production of actinorhodin in *Streptomyces coelicolor* by transcriptional analysis. *Scientific Reports*, 9(1), 11253. <https://doi.org/10.1038/s41598-019-46833-1>
- Lopatniuk, M., Myronovskiy, M., Nottebrock, A., Busche, T., Kalinowski, J., Ostash, B., ... Luzhetskyy, A. (2019). Effect of “ribosome engineering” on the transcription level and production of *S. albus* indigenous secondary metabolites. *Applied Microbiology and Biotechnology*, 103, 7097–7110. <https://doi.org/10.1007/s00253-019-10005-y>
- Love, M. I., Huber, W., & Anders, S. (2014). Moderated estimation of fold change and dispersion for RNA-seq data with DESeq2. *Genome Biology*, 15(12), 550. <https://doi.org/10.1186/s13059-014-0550-8>
- Lu, C., Zhang, X., Jiang, M., & Bai, L. (2016). Enhanced salinomycin production by adjusting the supply of polyketide extender units in *Streptomyces albus*. *Metabolic Engineering*, 35, 129–137. <https://doi.org/10.1016/j.ymben.2016.02.012>
- Martin, S. M., & Bushell, M. E. (1996). Effect of hyphal micromorphology on bioreactor performance of antibiotic-producing *Saccharopolyspora erythraea* cultures. *Microbiology*, 142(7), 1783–1788. <https://doi.org/10.1099/13500872-142-7-1783>
- McCormick, J. R., & Flärdh, K. (2012). Signals and regulators that govern *Streptomyces* development. *FEMS Microbiology Reviews*, 36(1), 206–231. <https://doi.org/10.1111/j.1574-6976.2011.00317.x>
- Myronovskiy, M., Rosenkranzer, B., Nadmid, S., Pujic, P., Normand, P., & Luzhetskyy, A. (2018). Generation of a cluster-free *Streptomyces albus* chassis strains for improved heterologous expression of secondary metabolite clusters. *Metabolic Engineering*, 49, 316–324. <https://doi.org/10.1016/j.ymben.2018.09.004>
- Natsume, M. (2016). Studies on bioactive natural products involved in the growth and morphological differentiation of microorganisms. *Journal of Pesticide Science*, 41(3), 96–101. <https://doi.org/10.1584/jpestics.116-03>
- Natsume, M., Tazawa, J., Yagi, K., Abe, H., Kondo, S., & Marumo, S. (1995). Structure-activity relationship of pamamycins: Effects of alkyl substituents. *The Journal of Antibiotics*, 48(10), 1159–1164. <https://doi.org/10.1038/ja.2008.118>
- Natsume, M., Yasui, K., Kondo, S., & Marumo, S. (1991). The structures of four new pamamycin homologues isolated from *Streptomyces alboniger*. *Tetrahedron Letters*, 32(26), 3087–3090. [https://doi.org/10.1016/0040-4039\(91\)80696-4](https://doi.org/10.1016/0040-4039(91)80696-4)
- O’Cleirigh, C., Casey, J. T., Walsh, P. K., & O’Shea, D. G. (2005). Morphological engineering of *Streptomyces hygroscopicus* var. *geldanus*: Regulation of pellet morphology through manipulation of broth viscosity. *Applied Microbiology and Biotechnology*, 68(3), 305–310. <https://doi.org/10.1007/s00253-004-1883-0>
- R Core Team (2014). *R: A language and environment for statistical computing*. Vienna, Austria: R Foundation for Statistical Computing.
- Rebets, Y., Brötz, E., Manderscheid, N., Tokovenko, B., Myronovskiy, M., Metz, P., ... Luzhetskyy, A. (2015). Insights into the pamamycin biosynthesis. *Angewandte Chemie-International Edition*, 127(7), 2309–2313. <https://doi.org/10.1002/anie.201408901>
- Ren, X.-D., Xu, Y.-J., Zeng, X., Chen, X.-S., Tang, L., & Mao, Z.-G. (2015). Microparticle-enhanced production of ϵ -poly-L-lysine in fed-batch fermentation. *RSC Advances*, 5(100), 82138–82143. <https://doi.org/10.1039/C5RA14319E>
- Saito, N., Xu, J., Hosaka, T., Okamoto, S., Aoki, H., Bibb, M. J., & Ochi, K. (2006). EShA accentuates ppGpp accumulation and is conditionally required for antibiotic production in *Streptomyces coelicolor* A3(2). *Journal of Bacteriology*, 188(13), 4952–4961. <https://doi.org/10.1128/JB.00343-06>
- Santamaría, R., & Pierre, P. (2012). Voronto: Mapper for expression data to ontologies. *Bioinformatics*, 28(17), 2281–2282. <https://doi.org/10.1093/bioinformatics/bts428>
- Schneider, C. A., Rasband, W. S., & Eliceiri, K. W. (2012). NIH Image to ImageJ: 25 years of image analysis. *Nature Methods*, 9(7), 671–675. <https://doi.org/10.1038/nmeth.2089>
- Sehgal, S. N., Baker, H., & Vézina, C. (1975). Rapamycin (AY-22, 989), a new antifungal antibiotic. II. Fermentation, isolation and characterization. *The Journal of Antibiotics*, 28(10), 727–732. <https://doi.org/10.7164/antibiotics.28.727>
- Traag, B. A., & van Wezel, G. P. (2008). The SsgA-like proteins in actinomycetes: Small proteins up to a big task. *Antonie Van Leeuwenhoek*, 94(1), 85–97. <https://doi.org/10.1007/s10482-008-9225-3>
- Vézina, C., Kudelski, A., & Sehgal, S. (1975). Rapamycin (AY-22, 989), a new antifungal antibiotic. I. Taxonomy of the producing streptomycete and isolation of the active principle. *The Journal of Antibiotics*, 28(10), 721–726. <https://doi.org/10.7164/antibiotics.28.721>
- Walisko, R., Krull, R., Schrader, J., & Wittmann, C. (2012). Microparticle based morphology engineering of filamentous microorganisms for industrial bio-production. *Biotechnology Letters*, 34(11), 1975–1982. <https://doi.org/10.1007/s10529-012-0997-1>
- Walisko, J., Vernen, F., Pommerehne, K., Richter, G., Terfehr, J., Kaden, D., ... Krull, R. (2017). Particle-based production of antibiotic rebeccamycin with *Lechevalieria aerocolonigenes*. *Process Biochemistry*, 53, 1–9. <https://doi.org/10.1016/j.procbio.2016.11.017>
- Wang, H., Zhao, G., & Ding, X. (2017). Morphology engineering of *Streptomyces coelicolor* M145 by sub-inhibitory concentrations of antibiotics. *Scientific Reports*, 7(1), 13226. <https://doi.org/10.1038/s41598-017-13493-y>
- Warnes, M. G. R., Bolker, B., Bonebakker, L., & Gentleman, R. (2016). *Package ‘gplots’*. Various R programming tools for plotting data.
- van Wezel, G. P., Krabben, P., Traag, B. A., Keijser, B. J., Kerste, R., Vijgenboom, E., ... Kraal, B. (2006). Unlocking *Streptomyces* spp. for use as sustainable industrial production platforms by morphological engineering. *Applied and Environmental Microbiology*, 72(8), 5283–5288. <https://doi.org/10.1128/AEM.00808-06>
- van Wezel, G. P., & McDowall, K. J. (2011). The regulation of the secondary metabolism of *Streptomyces*: New links and experimental

- advances. *Natural Product Reports*, 28(7), 1311–1333. <https://doi.org/10.1039/c1np00003a>
- van Wezel, G. P., van der Meulen, J., Kawamoto, S., Luiten, R. G., Koerten, H. K., & Kraal, B. (2000a). *ssgA* is essential for sporulation of *Streptomyces coelicolor* A3 (2) and affects hyphal development by stimulating septum formation. *Journal of Bacteriology*, 182(20), 5653–5662.
- van Wezel, G. P., van der Meulen, J., Taal, E., Koerten, H., & Kraal, B. (2000b). Effects of increased and deregulated expression of cell division genes on the morphology and on antibiotic production of *Streptomyces*. *Antonie Van Leeuwenhoek*, 78(3-4), 269–276. <https://doi.org/10.1023/a:1010267708249>
- Xia, X., Lin, S., Xia, X.-X., Cong, F.-S., & Zhong, J.-J. (2014). Significance of agitation-induced shear stress on mycelium morphology and lavendamycin production by engineered *Streptomyces flocculus*. *Applied Microbiology and Biotechnology*, 98(10), 4399–4407. <https://doi.org/10.1007/s00253-014-5555-4>
- Xu, H., Chater, K. F., Deng, Z., & Tao, M. (2008). A cellulose synthase-like protein involved in hyphal tip growth and morphological differentiation in *Streptomyces*. *Journal of Bacteriology*, 190(14), 4971–4978. <https://doi.org/10.1128/JB.01849-07>
- Zaburannyi, N., Rabyk, M., Ostash, B., Fedorenko, V., & Luzhetskyy, A. (2014). Insights into naturally minimised *Streptomyces albus* J1074 genome. *BMC Genomics*, 15(1), 97.
- Zhang, Y., Wang, M., Tian, J., Liu, J., Guo, Z., Tang, W., & Chen, Y. (2020). Activation of paulomycin production by exogenous γ -butyrolactone signaling molecules in *Streptomyces albidoflavus*. *Applied Microbiology and Biotechnology*, 104(1), J1074–J1705. <https://doi.org/10.1007/s00253-019-10329-9>

SUPPORTING INFORMATION

Additional supporting information may be found online in the Supporting Information section.

How to cite this article: Kuhl M, Gläser L, Rebets Y, et al. Microparticles globally reprogram *Streptomyces albus* toward accelerated morphogenesis, streamlined carbon core metabolism, and enhanced production of the antituberculosis polyketide pamamycin. *Biotechnology and Bioengineering*. 2020;117:3858–3875. <https://doi.org/10.1002/bit.27537>